PV Model Parameters Extraction using Opposition-Based Learning Flow Direction Algorithm

P. Siva Deepthi*‡, R. Kiranmayi**

*Department of EEE, Research Scholar, JNTU Anantapur, Anantapurumu, 515002

** Department of EEE, Professor, JNTU Anantapur, Anantapurumu, 515002

(sivadeepthi.reddy@gmail.com, kiranmayi0109@gmail.com)

‡ Corresponding Author: P. Siva Deepthi, JNTU Anantapur, Anantapurumu, 515002, Tel: +91 7680924149,

sivadeepthi.reddy@gmail.com

Received: 07.09.2023 Accepted:10.12.2023

Abstract – In this article, an Opposition Flow Direction Algorithm (OFDA) is used to extract the parameters of Photovoltaic (PV) Models. The Flow Direction Algorithm (FDA) is a unique variant of physics inspired algorithm. The D8 approach was used to determine how to mimic water flow into low-elevation areas, which was developed to simulate water flow into low-elevation areas based on the flow of water into neighbouring areas and the slope of those flows. The problem with the FDA is that it converges slowly and gets stuck on local minima too frequently. This article proposes an Opposition-Based Learning (OBL) for the FDA to improve exploration-exploitation balance, accelerate global convergence, and prevent local optima. Also, OFDA is used to extract the parameters of different PV cell models with the experimental data. Parameter extraction has been done for the RTC France PV cell and Photowatt-PWP 201 PV module to show the effectiveness of the proposed methodology. Simulations using MATLAB software have shown that the simulated I–V characteristics obtained using the extracted parameters agree with the experimental I–V values. Extensive theoretical and empirical investigation indicates that OFDA outperforms state-of-the-art precision, consistency, and efficiency more than OLGBO, IMFOL, FDA, and other algorithms.

Keywords: Parameter extraction, PV models, opposition-based learning, flow direction algorithm, mathematical modelling, optimization methods.

1. Introduction

Since electricity demand is rising exponentially and fossil fuels are decreasing, all the countries have focused on efficient Renewable Energy (RE) development and incorporation into the electric power grids in recent decades [1, 2]. There has been a remarkable uptick in using RE sources, comprising wind and solar power. Solar power is often recognized as the most significant RE resource for producing electrical energy, especially compared to conventional energy sources [3]. The most common use of solar power is the production of electricity by PV models [4]. Employing accurate PV models is crucial when describing a PV system's nonlinear I-V characteristics [5].

Several practical equivalent circuits, such as the SDM, DDM, and PVM, characterize the nonlinear I-V characteristics. Operating conditions like faults and aging of PV models can change the nonlinear I-V characteristics. The efficiency of PV models can be enhanced by extracting the exact parameters from the available data [6]. Parameters from the PV model may be utilized to monitor the system's health and spot any problems [7]. Because of these reasons, the researchers attempted to extract the PV model parameters and utilize these values to investigate the performance of their PV models. Again, these parameter values are also employed for Maximum PowerPoint Tracking Techniques (MPPT) [8, 9, 10]. Nevertheless, the PV models are nonlinear and non-convex implicit equations, which present challenges and obstacles to the solution techniques.

Determination of exact parameters is significant to obtain the efficient performance of PV models. Thus, getting the optimal PV model parameters is an optimization issue that can be solved using efficient optimization approaches [11-12]. The extraction of exact parameters for the associated unknown characteristics of PV models has been the subject of many studies [3].

With the emergence of population-based evolutionary, nature, and physics-inspired algorithms and their modifications, significant progress has been made in extracting parameters from PV models. These algorithms include: Improved Adaptive DE (IADE) [13], Particle Swarm Optimization (PSO) [14], adaptive Differential Evolution Technique (DET) [15], Time Varying Acceleration Coefficients PSO (TVACPSO) [16], Gravitational Search Algorithm (GSA) [17], Simplified Bird Mating Optimizer (SBMO) [18], Modified Simplified Swarm Optimization (MSSO) [19], Improved JAYA (IJAYA) [20], Quantum PSO (QPSO) [21], Improved Shuffled Complex Evolution (ISCE) [22], Multiple Learning Backtracking Search Algorithm (MLBSA) [23], Symbiotic Organisms Search (SOS) [24], Bacterial Foraging Optimization (BFO) [25], Coyote Optimization Algorithm (COA) [26], Performance-Guided JAYA (PGJAYA) [27], Modified Nelder-Mead Algorithm (MNMA) [28], Improved Teaching-Learning-Based Optimization (ITLBO) [29], Modified JAYA (MJA) [30], Self-adaptive Ensemble-based Differential Evolution (SEDE) [31], Grey Wolf Optimizer and Cuckoo Search (GWOCS) [32], Logistic Chaotic JAYA (LCJAYA) [33], Harris Hawks Optimization (HHO) and their modifications such as Diversification-enriched HHO with Chaotic Drifts (EHHO), Boosted HHO (BHHO) and Whippy HHO (WHHO) [34 – 37], Enhanced Adaptive DE (EJADE) [38], Marine Predators Algorithm (MPA) [39, 40], Refraction-Learning-Based Whale Optimization Algorithm (RLWOA) [41], a novel dynamic sine-cosine mechanism (DSCSE) [42], a novel heterogeneous DE (HDE) [43], a Modified Salp Swarm Algorithm (MSSA) [44], an Orthogonal Learning Gradient-Based Optimization (OLGBO) [45], Improved Moth Flame Algorithms with Local Escape Operators (IMFOL) [46], Slime Mould Algorithm (SMA) [47], Electromagnetism-like (IEM) [48], Spiral-Based Chaos Chicken Swarm Optimization (SCCSO) [49], Innovative Optimization Algorithm (INFO) [1].

A potent physics-based heuristic approach to global optimization, the Flow Direction Algorithm (FDA), was developed in 2021 [51]. It has an excellent global search capability, and its fundamental control is simpler and easier to implement. As a result of these benefits, the FDA algorithm and its modifications have found widespread use in various engineering applications [52–55]. There are still problems with the FDA despite its above-average performance. This article presents a modified Flow Direction Algorithm (FDA) based on OBL to improve the basic FDA's searchability, prevent it from encountering many local minima beneath the searching space, and provide more accurate search results.

The paper's main contributions are briefly summarized here:

- OFDA is utilized for the PV model parameter extraction with SDM, DDM, and PVM to test the efficacy and reliability of the OFDA method.
- The OFDA was feasible and thriving in the extraction parameters of various PV models, as shown by the comparable and statistically significant experimental findings.

2. Modelling of PV Modules and Problem Formulation

Many mathematical models in research explain the current-voltage behaviour of PV modules; in actuality, SDM, DDM, and PVM are predominant. These models are briefly described here as a mathematical approach to the corresponding issue.

2.1. Single Diode Model (SDM)

The SDM has seen extensive application in depicting solar cells' static characteristics. Figure 1 [24, 32] is a circuit model describing the essential circuitry, and the computation of the output current is shown below [24, 32].

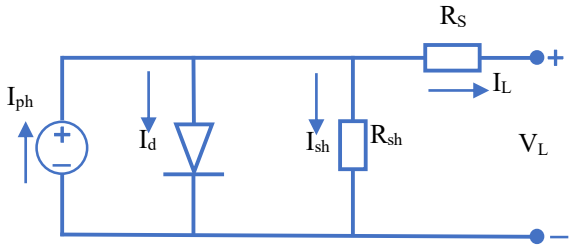


Fig. 1. Schematics diagram of SDM.

$$I_L=I_{ph}-I_d-I_{sh} \quad \dots (1)$$

where I_L is the output current, I_{ph} is the photocurrent, I_d is the diode current, and I_{sh} is the shunt resistor current.

$$I_d=I_o\left[\exp\left(\frac{V_L+I_LR_s}{n\times V_t}\right)-1\right] \quad \dots (2)$$

where "k is the constant of the Boltzmann (1.38065030×10-23 J/k), q is the electron charge (1.60217646×10-19 C) [32]", I_o is the reverse saturation current of diode, V_L is the output voltage, R_s is the series resistance, V_t is the junction thermal voltage obtained by Eq. (3).

$$V_t=\frac{kT}{q} \quad \dots (3)$$

The Ish is the shunt resistor current is calculated as follows.

$$I_L=I_{ph}-I_o\left[\exp\left(\frac{q.(V_L+I_LR_s)}{n.k.T}\right)-1\right]-\frac{V_L+I_LR_s}{R_{sh}} \quad \dots (4)$$

where I_L is the output current, I_{ph} is the photocurrent, I_d is the diode current, and I_{sh} is the shunt resistor current.

2.2. Double Diode Model (DDM)

The DDM has seen extensive application to depict solar cells' static features because of its accuracy and simplicity. Figure 2 [24, 32] describes the corresponding circuit model; the calculated output current is below [24, 32].

$$I_L=I_{ph}-I_{d1}-I_{d2}-I_{sh} \quad \dots (5)$$

$$I_{d1}=I_{o1}\times\left[\exp\left(\frac{V_L+I_LR_s}{n_1\times V_t}\right)-1\right] \text{ and } I_{d2}=I_{o2}\times\left[\exp\left(\frac{V_L+I_LR_s}{n_2\times V_t}\right)-1\right] \quad \dots (6)$$

where I_{o1} and I_{o2} represent the diffusion and saturation currents, respectively. n_1 and n_2 represent the diffusion and recombination diode ideality factors, respectively.

$$I_L=I_{ph}-I_{o1}\left[\exp\left(\frac{q.(V_L+I_LR_s)}{n_1.k.T}\right)-1\right]-I_{o2}\left[\exp\left(\frac{q.(V_L+I_LR_s)}{n_2.k.T}\right)-1\right]-\frac{V+I_LR_s}{R_{sh}} \quad \ldots (7)$$

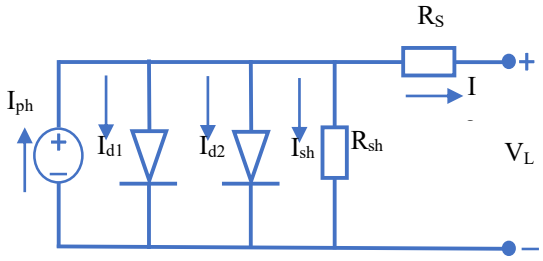


Fig. 2. Schematics diagram of DDM.

2.3. Photovoltaic Module Model (PMM)

The utilization of the PVM has been prevalent in illustrating the static characteristic of solar cells due to its precision and straightforwardness. Figure 3 [24, 32] displays the corresponding circuit model, and the computation of the output current is summarized below [24, 32].

$$I_L=N_pI_{ph}-N_pI_o\times\left[\exp\left(\frac{1}{V_t}\left(\frac{V_L}{N_s}+\frac{IR_s}{N_p}\right)\right)-1\right]-\frac{N_p}{R_p}\left(\frac{V_L}{N_s}+\frac{IR_s}{N_p}\right) \quad \ldots (8)$$

where N_p is the number of solar cells in parallel, and N_S is the number of solar cells in series. I_L is the output current, I_{ph} is the photocurrent, I_d is the diode current, and I_{sh} is the shunt resistor current.

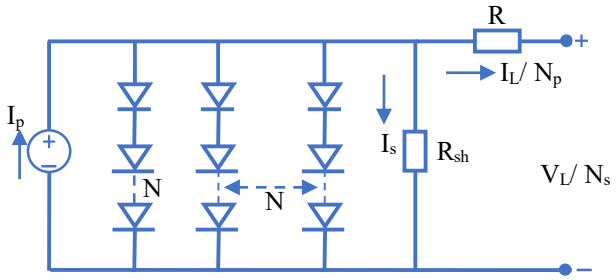


Fig. 3. Schematics diagram of PVM.

2.4. Objective Function

The best parameters are extracted to lower the difference between actual and simulation data. The problem of finding the correct parameters for PV models is often remade as an optimization problem. Eq. (11), (12) and (13) [24, 32] show the error function for each set of actual and simulated current data points for the single, double-diode, and PV models [24, 32].

$$f(V_L, I_L, X_{SDM})=I_{ph}-I_o\left[\exp\left(\frac{q.(V_L+I_LR_s)}{n.k.T}\right)-1\right]-\frac{V_L+I_LR_s}{R_{sh}}-I_L \quad \ldots (9)$$

$$f(V_L, I_L, X_{DDM})=I_{ph}-I_{o1}\left[\exp\left(\frac{q.(V_L+I_LR_s)}{n_1.k.T}\right)-1\right]-I_{o2}\left[\exp\left(\frac{q.(V_L+I_LR_s)}{n_2.k.T}\right)-1\right]-\frac{V_L+I_LR_s}{R_{sh}}-I_L \quad \ldots (10)$$

$$f(V_L, I_L, X_{PVM})=N_pI_{ph}-N_pI_o\times\left[\exp\left(\frac{1}{V_t}\left(\frac{V_L}{N_s}+\frac{IR_s}{N_p}\right)\right)-1\right]-\frac{N_p}{R_p}\left(\frac{V_L}{N_s}+\frac{IR_s}{N_p}\right) \quad \ldots (11)$$

Objective Function of the problem is shown below.

$$RMSE=\sqrt{\frac{1}{N}\sum_{i=1}^{N}P(V_e,I_e,X)} \quad \ldots (12)$$

3. Flow Direction Algorithms

3.1. Flow Direction Algorithm

Karami [51] was used the D8 technique to develop the Flow Direction Algorithm (FDA) in 2021. The D8 algorithm determines the direction of water flow in a drainage basin after transforming the rainfall into runoff. Figure 4 [51] shows the basin outflow flow with the D8 technique. This method generates an original population in the drainage basin, which can also be considered the problem search space. Then, water flows are directed towards the lowest elevation area as much as possible, which can also be considered the best solution.

The initial location of flows is computed in the FDA as follows [51]:

$$X_Flow(i) = lb+rand\times(ub-lb) \quad \ldots (13)$$

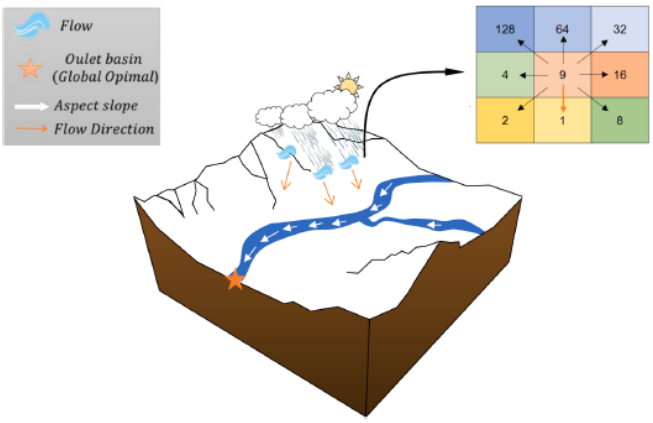


Fig. 4. Diagram of basin outflow flow with the D8 technique.

In addition to this, it is presumed that there are some β neighbourhood flows around each flow; the neighbouring flows are calculated as follows [51]:

$$Neighbour(j)=X_Flow(i)+\Delta\times randn \quad \ldots (14)$$

where a Neighbour(j) represents the neighbour's position, and Δ is the neighbourhood radius. The exploration will be limited to a small range if the value is minute; if the Δ value is significant, the exploration will open up the possibility of exploring a broad range. In this technique, to improve the probability of finding the closest to the optimal solutions (global search), search a wide range of search space that offers various solutions, and it is necessary for exploring a small

region of the search space containing several optimal solutions to find the optimal global solution (local search) more truthfully. If a global search process is enforced in the technique, the algorithm cannot discover the global optimum with the necessary precision; similarly, if a local approach is implemented, the algorithm gets stuck with local optima. If a global search process is enforced in the algorithm, the algorithm cannot discover the global optimum with the necessary precision; similarly, if a local approach is implemented, the algorithm gets stuck with local optima. In this technique, the value of Δ was linearly reduced from the highest value to the smallest value to maintain the balance between global and local search; now, the direction of Δ is towards a random position for more variation. The mathematical modelling of Δ as follows [51]:

$$\Delta=(\text{rand}\times X_{\text{rand}} - \text{rand} \times \text{X_Flow(i)})\times\|\text{X_Best} - \text{X_Flow}\|\times W \quad \ldots (15)$$

where *Xrand* is a random position, "*X_Best*" is the best position, and *W* is a nonlinear weight. This first one describes that *X_Flow (i)* moves to *Xrand*. For the next one, by changing iteration, *X_Flow(i)* is closed to *X_Best*, and the Euclidian distance between *X_Best* and *X_Flow(i)* is zero. The mathematical modelling of *W* is as follows [51]:

$$W=\left(\left(1-\frac{\text{iter}}{\text{Max_iter}}\right)^{(2\times\text{randn})}\right)\times\left(\text{rand}\times\frac{\text{iter}}{\text{Max_iter}}\right)\times\text{rand} \quad \ldots (16)$$

The changes of *W* while increasing the iterations are shown in Figure 5 [51]; this can avoid being stuck with local optima in the algorithm. All the water flows move with a velocity of *V* to the neighbour with the minimum fitness function.

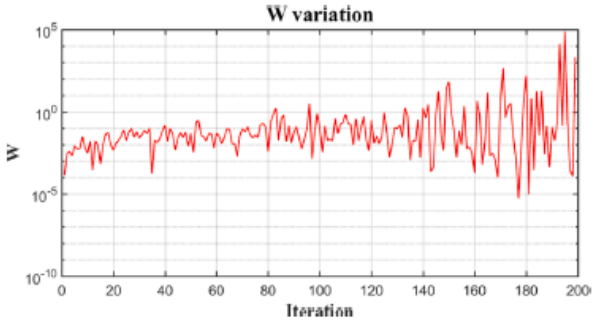


Fig. 5. The changes of W.

The velocity of the water flow to neighbour flows depends on its slope. The mathematical modelling of *V* is as follows [51]:

$$V=\text{randn}\times S_o \quad \ldots (17)$$

where S_o is the slope between the current and neighbour water flows; the *randn* generates numerous solutions and enhances global search capability. The following relation also determines the slope of i^{th} water flow to the neighbour j^{th} [51]:

$$S(i, j, d)=\frac{\text{Fitness_Flow(i)-Neighbor_Fitness(j)}}{\|\text{X_Flow(i,d)-Neighbor(j,d)}\|} \quad \ldots (18)$$

To find the new position of water flow, the mathematical modelling is as follows [51]:

$$\text{Flow_Xnew(i)=Flow_X(i)+V}\times\frac{\text{X_Flow(i)-Neighbor(j)}}{|\text{X_Flow(i)-Neighbor(j)}|} \quad \ldots (19)$$

The FDA algorithm picks a new flow randomly; if its fitness function is less than the current flow's, it will follow the same path; otherwise, it will follow the prevailing slope direction, analogous to the sink-filling process used to determine the water flow direction. Figure 6 [51] depicts the sink's location before and after being filled.

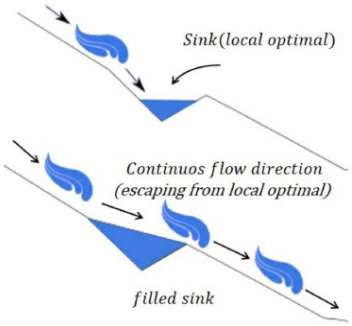


Fig. 6. Position of a sink before and after filling.

The subsequent relation may model the flow direction [51].

if Fitness_Flow(r)<Fitness_Flow(i)
Flow_Xnew(i)=X_Flow(i)+randn×(X_Flow(r)-X_Flow(i))
otherwise
Flow_Xnew(i)=X_Flow(i)+2randn×(X_Best-X_Flow(i)) … (20)

3.2. Opposition-Based Learning Flow Direction Algorithm

The global search process may speed up the algorithm's convergence, which can lead to bypassing the best solution in population-based optimization. In addition to guaranteeing sufficient convergence accuracy, the scope of the local search process is a critical factor in defining an algorithm's performance in terms of exploration and exploitation. However, algorithms need to strike a balance between discovery and use. To improve the basic FDA's searchability, prevent many local minima beneath the search space, acquire greater search capacity, and strike the right equilibrium between exploratory and exploitative search, researchers have developed an Opposition-Based Learning (OBL) technique [56, 57]. By searching in opposing directions, as in Opposition-Based Learning (OBL), it is more likely the problem's undiscovered optimum will be uncovered. When the optimal locations are opposite to the present solution, the OBL is particularly effective. Thus, in the current study, an OBL phase is included in the FDA to escape local optima when they get stuck and to investigate more fruitful parts of the search space. This idea proposes that not only does the solution but also its antithesis aid in the discovery process. Opposition-based learning may also lessen the computational burden [57]. The flowchart of the proposed OFDA is shown in Figure 7 [52]. The OBL algorithm's Pseudo code is below in Figure 8 [57].

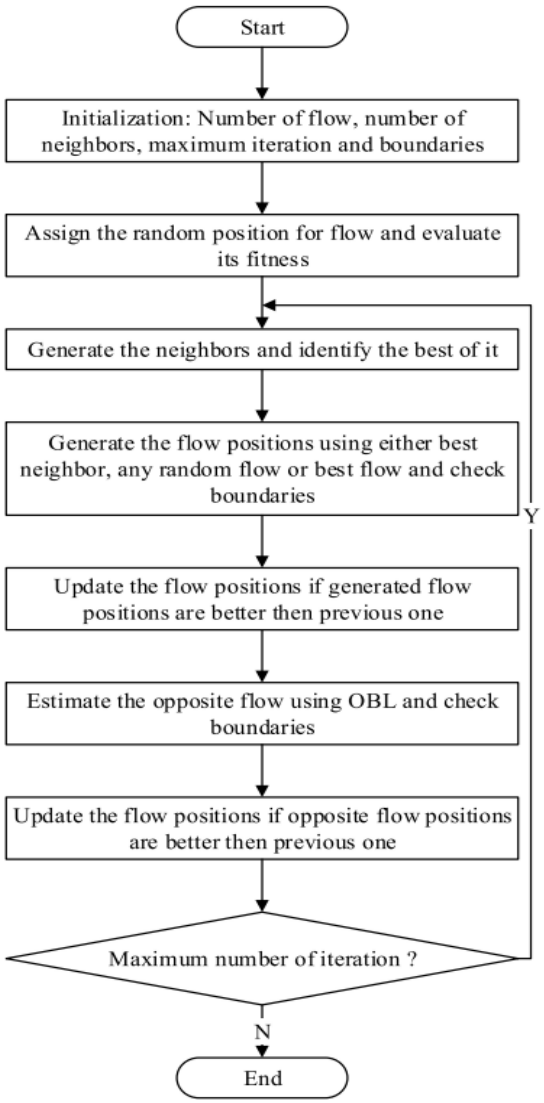


Fig. 7. Flowchart of the proposed approach.

Table 1. Pseudo code of OBL algorithm

for (all the flows)
  for (all the dimensions)
    $OP_{ij} = a_j + b_j - x_{ij}$
  end (all the dimensions)
end (all the flows)
Return $OP = [OP_{ij}]$

The proposed approach utilized the below formula [57] to get the opposite number."x̂" of a point x in the range (a, b) [57]. The Pseudo code of the OBL algorithm is shown in Figure 8 [57].

$$\hat{x} = a + b - x \quad \ldots (21)$$

where *a* and *b* are the values of lower and upper for "x̂". Extending this idea to the vectors of R_d yields the following [57]:

Let $X = (x_1, x_2, \ldots, x_d) \in R$

$X = x_1^*, x_2^*, \ldots, x_d^*$

$$x_i^* = (a_i + b_i - x_i), \text{ for } i = 1, 2..., d, \quad \ldots (22)$$

The Pseudo code of the OFDA algorithm is shown in Table 3.

4. Results and Discussions

The extraction of parameters of PV cells and modules has verified the effectiveness and robustness of OFDA. This issue is demonstrated in MATLAB R2021a and runs on the PC with 8 GB RAM and an 11th Gen Intel Core i5-11300H @ 3.10GHz processor.

The adopted OFDA is utilized for parameter extraction of various solar cells and PV modules like SDM, DDM, and PVM to analyze its effectiveness, verify its capability to address the problem, and evaluate its performance against well-established techniques like IJAYA [20], MLSBA [23], PGJAYA [27], EJADE [38], GWOCS [32], DSCSE [42], HDE [43], MSSA [44], OLGBO [45], and IMFOL [46]. "The measured data of commercial RTC France silicon solar cell under 1000 W/m2 at 33 °C and Photowatt-PWP201 under 1000 W/m2 at 45 °C utilized" from [1] and the specifications of the solar cells and PV modules are presented in Table 2.

Table 2. Minimum and maximum limits of each model

Parameter	SDM/DDM		Photowatt-PWP201	
	[LB	UB]	[LB	UB]
I_{ph}	[0	1]	[0	2]
I_{sd}, I_{sd1}, I_{sd2}	[0	1]	[0	50]
R_s	[0	0.5]	[0	2]
R_{sh}	[0	100]	[0	2000]
n, n_1, n_2	[0	2]	[0	50]

The proposed algorithm was executed for each solar cell and PV module 30 times independently, with each run having a maximum of 5000 iterations and a population size of 100. After running the algorithm for each solar cell and PV module, recording the results, like extracted parameter values, Minimum (Min), Maximum (Max), Avarage Value (Mean), and Standard Deviation (Std) values, were calculated based on the outcomes of the 30 independent runs.

The proposed OFDA's performance has been compared with the original FDA and other well-known algorithms. The proposed OFDA and FDA are performed with the same maximum number of iterations (max_it) 5000. After that, the proposed OFDA is compared with other well-known algorithms from the literature, such as IJAYA [20], MLSBA [23], PGJAYA [27], EJADE [38], GWOCS [32], DSCSE [42], HDE [43], MSSA [44], OLGBO [45], and IMFOL [46]. The comparison results will establish evidence of the algorithm's precision, efficiency, and competitiveness in optimizing the parameter extraction of solar cells and PV modules. First, the accuracy of different algorithms may be compared by looking at their minimum RMSE values. Each method's convergence accuracy and speed are then measured using statistical data and convergence curves.

Table 3. Pseudo code of OFDA algorithm

```
Initialize the search agents (X_Flow(i)) i = 1, . . ., n
Compute the fitness function and create a fitness matrix
Initialize the velocity of flows Vmin and Vmax
while it < itmax
        update the W using (Eq. 16)
        for (all the flows)
                for (all the neighbors)
                        Initialize neighborhood radius Δj; j = 1, . . ., β using (Eq. 15)
                        Initialize neighbor flows X_ neighbor
                        Compute the neighbor fitness function and create a fitness matrix
                end (all the neighbors)
                update the slope of neighbor using (Eq. 18)
                if neighbor fitness < flow fitness
                        update the velocity of each flow using (Eq. 17)
                        update the new flow using (Eq. 21)
                else
                        update the new flow using (Eq. 20)
                end
                update the best flow and fitness function
        end (all the flows)
        Algorithm of OBL
end (while)
```

4.1. Case 1: Single Diode Model (SDM):

The simulation outcomes are provided in Table 4, the optimal parameter values (I_{ph}, I_{sd}, R_s, R_{sh}, and n) and the values of RMSE attained by the original FDA, proposed OFDA, and other well-known algorithms, in which the minimum RMSE is marked in bold. In addition, it is clear from Table 4 that IJAYA [20], MLSBA [23], PGJAYA [27], EJADE [38], GWOCS [32], DSCSE [42], HDE [43], MSSA [44], OLGBO [45], and IMFOL [46], FDA, and OFDA produced the better RMSE value is 9.8602E-04, and GWOCS achieved the worst value of RMSE is 9.8607E-04. The convergence rate of the proposed OFDA and FDA, as in Figure 8 for the SDM model, OFDA has a quicker convergence rate than FDA.

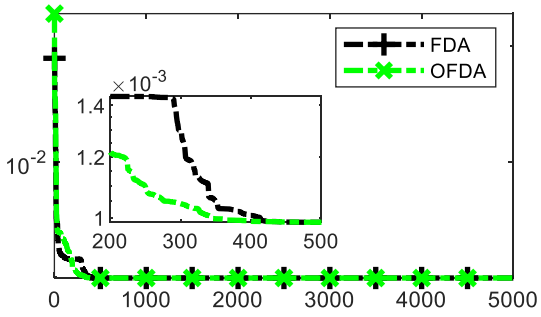


Fig. 8. The convergence curves of both the FDA and OFDA for the SDM model.

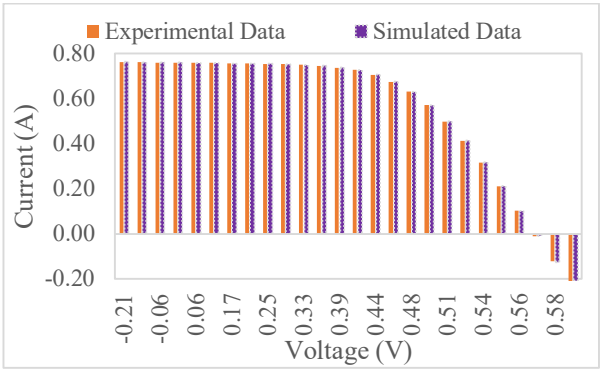


Fig. 9. (a) Current-Voltage (I-V) characteristics of SDM.

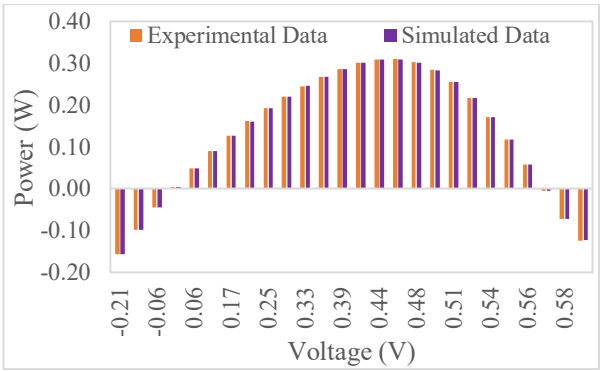


Fig. 9. (b) Power-Voltage (P-V) characteristics of SDM.

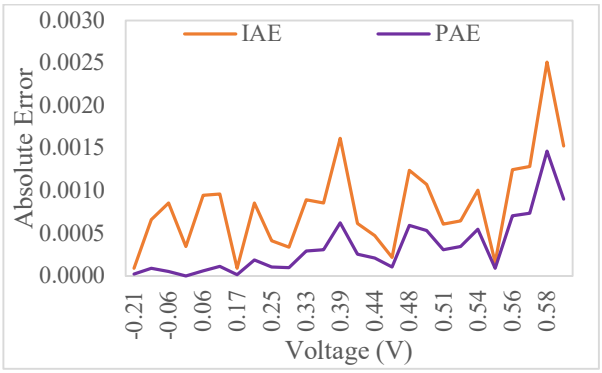


Fig. 9. (c) Individual absolute error (IAE).

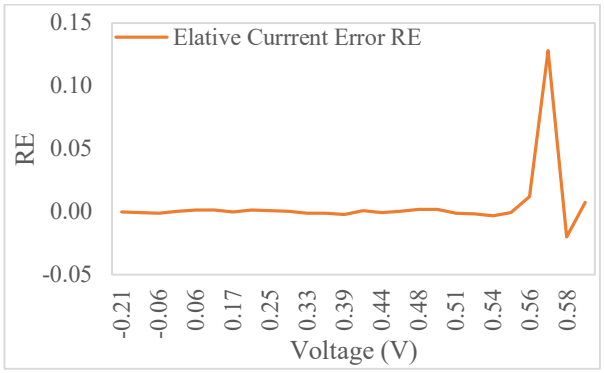


Fig. 9. (d) Relative error (RE)

Fig. 9. The error-index of the experimental and simulated current data for the SDM.

Table 4. The SDM results of extracted parameter values of OFDA and other well-known algorithms

Algorithm	I_{ph} (A)	I_{sd1} (A)	R_s(Ω)	R_p(Ω)	n	RMSE
IJAYA [20]	0.7608	3.2880E-01	0.0364	53.7595	1.4811	9.8603E-04
MLBSA [23]	0.7608	3.2302E-01	0.0364	53.7185	1.4812	**9.8602E-04**
PGJAYA [27]	0.7608	3.2300E-01	0.0364	53.7185	1.4812	**9.8602E-04**
EJADE [38]	0.7608	3.2300E-01	0.0364	53.7185	1.4812	**9.8602E-04**
GWOCS [32]	0.7608	3.2192E-01	0.0364	53.632	1.4808	9.8607E-04
DSCSE [42]	0.7608	3.2302E-07	0.0364	53.7185	1.4812	**9.8602E-04**
HDE [43]	0.7608	3.2302E-07	0.0364	53.7185	1.4812	**9.8602E-04**
MSSA [44]	0.7683	3.2620E-01	0.0367	54.2557	1.4958	9.86E-04
OLGBO [45]	0.7608	3.2302E-07	0.0364	53.7185	1.4812	**9.8602E-04**
IMFOL [46]	0.7608	3.2302E-07	0.0364	53.3719	1.4819	**9.8602E-04**
FDA	0.7608	3.2302E-07	0.0364	53.7185	1.4812	**9.8602E-04**
OFDA	0.7608	3.2302E-07	0.0364	53.7185	1.4812	**9.8602E-04**

Table 5. The SDM statistical results of OFDA and other well-known algorithms

Algorithm	Min	Max	Mean	Std
IJAYA [20]	9.8603E-04	1.0622E-03	9.9204E-04	1.4033E-05
MLBSA [23]	9.8602E-04	9.8602E-04	9.8602E-04	9.1461E-12
PGJAYA [27]	9.8602E-04	9.8602E-04	9.8602E-04	1.4485E-09
EJADE [38]	9.8602E-04	9.8602E-04	9.8602E-04	5.1300E-17
GWOCS [32]	9.8607E-04	9.9095E-04	9.8874E-04	2.4696E-06
DSCSE [42]	9.8602E-04	9.8603E-04	9.8602E-04	1.1321E-09
HDE [43]	9.8602E-04	9.8602E-04	9.8602E-04	4.5699E-17
MSSA [44]	9.86E-04	9.8700E-04	9.8500E-04	3.0100E-07
OLGBO [45]	9.2602E-04	1.0127E-03	9.8719E-04	4.9110E-06
IMFOL [46]	9.8602E-04	9.8977E-04	9.8705E-04	1.0207E-06
FDA	9.8602E-04	9.8602E-04	9.8602E-04	3.9760E-17
OFDA	9.8602E-04	9.8602E-04	9.8602E-04	**3.0905E-17**

Table 6. The SDM absolute error (IAE) values

Experimental Data		Simulated Data		Simulated Data	
V (V)	I (A)	Isim (A)	I_IAE (A)	P (W)	P_IAE (W)
-0.2057	0.7640	0.76408770	8.7704E-05	-0.157173	1.8041E-05
-0.1291	0.7620	0.76266309	6.6309E-04	-0.098460	8.5604E-05
-0.0588	0.7605	0.76135531	8.5531E-04	-0.044768	5.0292E-05
0.0057	0.7605	0.76015399	3.4601E-04	0.004333	1.9723E-06
0.0646	0.7600	0.75905521	9.4479E-04	0.049035	6.1034E-05
0.1185	0.7590	0.75804234	9.5766E-04	0.089828	1.1348E-04
0.1678	0.7570	0.75709165	9.1654E-05	0.127040	1.5379E-05
0.2132	0.7570	0.75614136	8.5864E-04	0.161209	1.8306E-04
0.2545	0.7555	0.75508687	4.1313E-04	0.192170	1.0514E-04
0.2924	0.7540	0.75366388	3.3612E-04	0.220371	9.8282E-05
0.3269	0.7505	0.75139097	8.9097E-04	0.245630	2.9126E-04
0.3585	0.7465	0.74735385	8.5385E-04	0.267926	3.0611E-04
0.3873	0.7385	0.74011722	1.6172E-03	0.286647	6.2635E-04
0.4137	0.7280	0.72738222	6.1778E-04	0.300918	2.5557E-04
0.4373	0.7065	0.70697265	4.7265E-04	0.309159	2.0669E-04
0.4590	0.6755	0.67528015	2.1985E-04	0.309954	1.0091E-04
0.4784	0.6320	0.63075827	1.2417E-03	0.301755	5.9404E-04
0.4960	0.5730	0.57192836	1.0716E-03	0.283676	5.3153E-04
0.5119	0.4990	0.49960702	6.0702E-04	0.255749	3.1073E-04
0.5265	0.4130	0.41364879	6.4879E-04	0.217786	3.4159E-04
0.5398	0.3165	0.31751011	1.0101E-03	0.171392	5.4526E-04
0.5521	0.2120	0.21215494	1.5494E-04	0.117131	8.5542E-05
0.5633	0.1035	0.10225131	1.2487E-03	0.057598	7.0339E-04
0.5736	-0.0100	-0.00871754	1.2825E-03	-0.005000	7.3562E-04
0.5833	-0.1230	-0.12550741	2.5074E-03	-0.073208	1.4626E-03
0.5900	-0.2100	-0.20847233	1.5277E-03	-0.122999	9.0133E-04

Table 5 shows the root-mean-square error (RMSE) minimum, maximum, mean, and standard deviation throughout 30 iterations to evaluate the OFDA's effectiveness. As expected, the OFDA performs the best for Mean and Std compared with other well-known algorithms. The Mean of the OFDA is identical to the MLSBA [23], PGJAYA [27], EJADE [38], DSCSE [42], HDE [43], and FDA. The Std. of the OFDA is very close to the EJADE [38], HDE [43], and FDA but superior to other well-known algorithms. According to the results reported above, we may conclude that OFDA is competent to be an effective technique for extracting the SDM parameters.

The OFDA-obtained SDM optimum parameters are shown in Table 6; finally, the simulated I-V and P-V data are computed using these values. Table 6 displays the Individual Absolute Error (IAE), whereas Figure 9 displays the relative characteristic curves between the observed and calculated data. Table 6 shows that the corresponding IAE values for current are less than 1.4626E-03, and IAE values for power are less than 2.5074E-03. Current and power levels calculated using the OFDA are demonstrated to agree with experimental measurements in Figure 9. All of this evidence points to the specified parameters being correct.

4.2. Case 2: Double Diode Model (DDM):

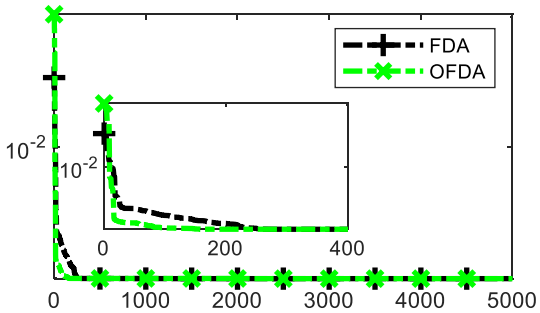


Fig. 10. The convergence curves of both the FDA and OFDA for the DDM model.

The simulation outcomes are provided in Table 7, the optimal parameter values (I_{ph}, I_{sd1}, I_{sd2}, R_s, R_{sh}, n_1, and n_2) and the values of RMSE attained by the original FDA, proposed OFDA and other well-known algorithms, in which the minimum RMSE is marked in bold. In addition, it is clear from

Table 7 that EJADE [38], HDE [43], OLGBO [45], FDA, and OFDA produced the better RMSE value of 9.8248E-04, and GWOCS attained the worst RMSE value of 9.8334E-04. The convergence rate of the proposed OFDA and FDA, as in Figure 10 for the DDM model, OFDA has a quicker convergence rate than FDA.

Table 8 shows the root-mean-squared error (RMSE) minimum, maximum, mean, and standard deviation throughout 30 iterations to evaluate the OFDA's effectiveness. As expected, the OFDA performs the best for Mean and Std compared with other well-known algorithms. The Mean of the OFDA is 9.8419E-04, superior to the IJAYA [20], FDA, EJADE [38], HDE [43], AND worse than the MLBSA [27], DSCSE [42], PGJAYA [27], IMFOL [46], MSSA [44], GWOCS [32], OLGBO [45]. The Std. of the OFDA is very close to the MLSBA [23], EJADE [38], DSCSE [42], HDE [43], MSSA [44], and FDA, but superior to the all-other well-known algorithms. According to the results reported above, we may conclude that OFDA has the potential to be an effective technique for identifying the DDM parameters.

Table 7. The DDM results of extracted parameter values of OFDA and other well-known algorithms

Algorithm	I_{ph} (A)	I_{sd1} (A)	R_s (Ω)	R_{sh} (Ω)	n_1	I_{sd2} (A)	n_2	RMSE
IJAYA [20]	0.7601	5.0445E-03	0.0376	77.8519	1.2186	7.5094E-01	1.6247	9.8249E-04
MLBSA [23]	0.7608	2.2728E-01	0.0367	55.4612	1.4545	7.3835E-01	2.0000	9.8249E-04
PGJAYA [27]	0.7608	2.1031E-01	0.0368	55.8135	1.4450	8.8534E-01	2.0000	9.8263E-04
EJADE [38]	0.7608	2.2600E-01	0.0367	55.4854	1.4510	7.4930E-01	2.0000	**9.8248E-04**
GWOCS [32]	0.7608	5.3772E-01	0.0367	54.7331	2.0000	2.4855E-01	1.4588	9.8334E-04
DSCSE [42]	0.7608	6.9804E-07	0.0367	55.3750	2.0000	2.3184E-07	1.4532	9.8251E-04
HDE [43]	0.7608	7.4935E-07	0.0367	55.4854	2.0000	2.0260E-07	1.4510	**9.8248E-04**
MSSA [44]	0.7608	9.7310E-01	0.0369	53.8368	1.9213	1.6790E-01	1.4281	9.83E-04
OLGBO [45]	0.7608	7.4391E-07	0.0367	55.4710	2.0000	2.2660E-07	1.4513	**9.8248E-04**
IMFOL [46]	0.7608	7.6632E-07	0.0367	55.6567	2.0000	2.2515E-07	1.4508	9.8253E-04
FDA	0.7608	2.2597E-07	0.0367	55.4854	1.4510	7.4935E-07	2.0000	**9.8248E-04**
OFDA	0.7608	2.2597E-07	0.0367	55.4854	1.4510	7.4935E-07	2.0000	**9.8248E-04**

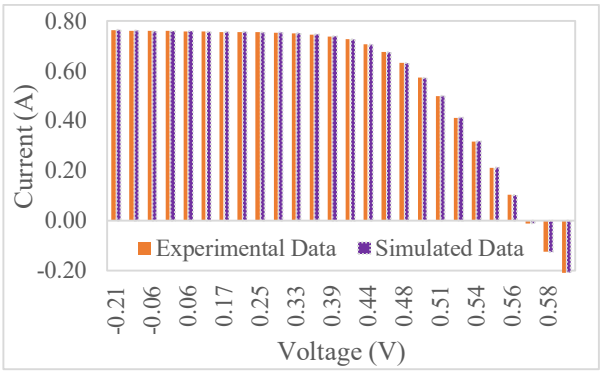


Fig. 11. (a) Current-Voltage (I-V) characteristics of SDM.

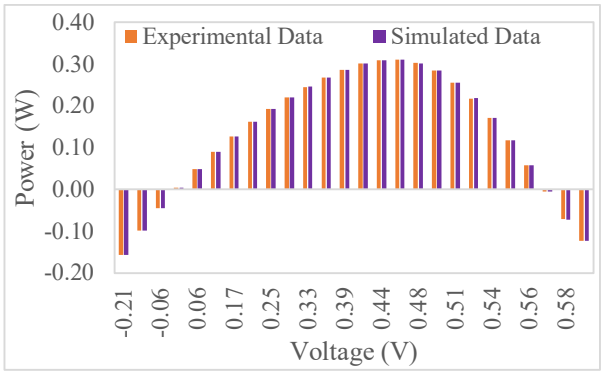


Fig. 11. (b) Power-Voltage (P-V) characteristics of DDM

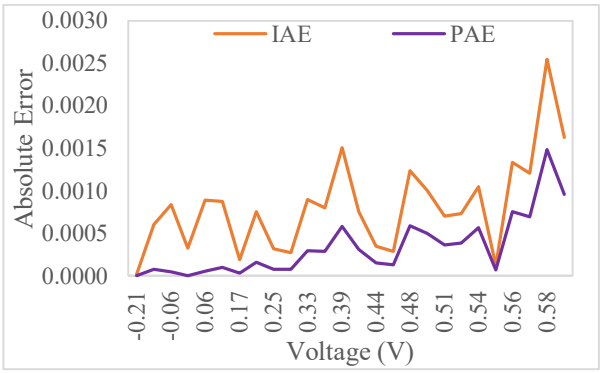


Fig. 11. (c) Individual absolute error (IAE).

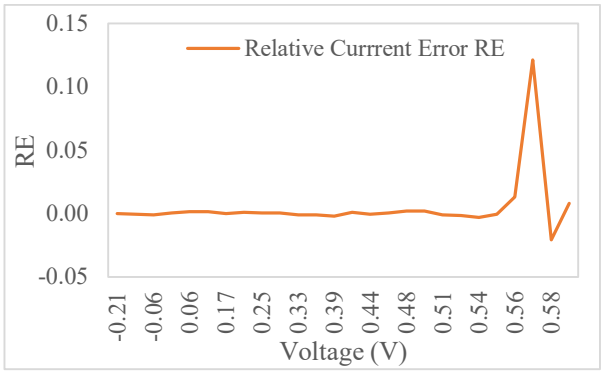


Fig. 11. (d) Relative error (RE).

Fig. 11. The error index of the experimental and simulated current data for the DDM.

The OFDA-obtained DDM optimum parameters are shown in Table 9; finally, the simulated I-V and P-V data are computed using these values. Table 9 displays the Individual Absolute Error (IAE), whereas Figure 11 displays the relative characteristic curves between the observed and calculated data. Table 9 shows that the corresponding IAE values for current are less than 1.4836E-03, and IAE values for power are less than 2.5434E-03. Current and power levels calculated using the OFDA are demonstrated to agree with experimental measurements in Figure 11.

Table 8. The DDM statistical results of OFDA and other well-known algorithms

Algorithm	Min	Max	Mean	Std
IJAYA [20]	9.8293E-04	1.4055E-03	1.0269E-03	9.8325E-05
MLBSA [23]	9.8249E-04	9.8798E-04	9.8518E-04	1.3482E-06
PGJAYA [27]	9.8263E-04	9.9499E-04	9.8582E-04	2.5375E-06
EJADE [38]	9.8248E-04	9.8602E-04	9.8363E-04	1.3600E-06
GWOCS [32]	9.8334E-04	1.0017E-03	9.9411E-04	9.5937E-06
DSCSE [42]	9.8251E-04	9.8776E-04	9.8525E-04	1.2792E-06
HDE [43]	9.8248E-04	9.8602E-04	9.8415E-04	1.6726E-06
MSSA [44]	9.8300E-04	9.9900E-04	9.9400E-04	1.4900E-06
OLGBO [45]	9.8249E-04	1.2784E-03	9.9567E-04	5.3497E-05
IMFOL [46]	9.8253E-04	9.9596E-04	9.8768E-04	3.2268E-06
FDA	9.8248E-04	9.8602E-04	9.8331E-04	1.5216E-06
OFDA	9.8248E-04	9.8602-04	9.8419E-04	**1.43870-06**

Table 9. The results of absolute error (IAE) on the single diode DDM.

Experimental Data		Simulated Data		Simulated Data	
V (V)	I (A)	Isim (A)	I_IAE (A)	P (W)	P_IAE (W)
-0.2057	0.7640	0.76398341	1.6587E-05	-0.157151	3.4120E-06
-0.1291	0.7620	0.76260410	6.0410E-04	-0.098452	7.7989E-05
-0.0588	0.7605	0.76133770	8.3770E-04	-0.044767	4.9257E-05
0.0057	0.7605	0.76017379	3.2621E-04	0.004333	1.8594E-06
0.0646	0.7600	0.75910768	8.9232E-04	0.049038	5.7644E-05
0.1185	0.7590	0.75812142	8.7858E-04	0.089837	1.0411E-04
0.1678	0.7570	0.75718861	1.8861E-04	0.127056	3.1649E-05
0.2132	0.7570	0.75624361	7.5639E-04	0.161231	1.6126E-04
0.2545	0.7555	0.75517730	3.2270E-04	0.192193	8.2127E-05
0.2924	0.7540	0.75372235	2.7765E-04	0.220388	8.1184E-05
0.3269	0.7505	0.75139913	8.9913E-04	0.245632	2.9393E-04
0.3585	0.7465	0.74730144	8.0144E-04	0.267908	2.8732E-04
0.3873	0.7385	0.74001066	1.5107E-03	0.286606	5.8508E-04
0.4137	0.7280	0.72724695	7.5305E-04	0.300862	3.1154E-04
0.4373	0.7065	0.70685030	3.5030E-04	0.309106	1.5319E-04
0.4590	0.6755	0.67521054	2.8946E-04	0.309922	1.3286E-04
0.4784	0.6320	0.63076076	1.2392E-03	0.301756	5.9285E-04
0.4960	0.5730	0.57199473	1.0053E-03	0.283709	4.9861E-04
0.5119	0.4990	0.49970613	7.0613E-04	0.255800	3.6147E-04
0.5265	0.4130	0.41373367	7.3367E-04	0.217831	3.8628E-04
0.5398	0.3165	0.31754621	1.0462E-03	0.171411	5.6474E-04
0.5521	0.2120	0.21212300	1.2300E-04	0.117113	6.7906E-05
0.5633	0.1035	0.10216328	1.3367E-03	0.057549	7.5298E-04
0.5736	-0.0100	-0.00879175	1.2082E-03	-0.005043	6.9305E-04
0.5833	-0.1230	-0.12554343	2.5434E-03	-0.073229	1.4836E-03
0.5900	-0.2100	-0.20837159	1.6284E-03	-0.122939	9.6076E-04

4.3. Case 3: Photovoltaic Module Model (PMM)

The simulation outcomes are provided in Table 10, the optimal parameter values (I_{ph}, I_{sd}, R_s, R_{sh}, and n) and the values of RMSE attained by the original FDA, proposed OFDA, and other well-known algorithms, in which the minimum RMSE is marked in bold. In addition, it is clear from Table 10 that all the well-known algorithms, along with the FDA and OFDA, produced the best RMSE value of 2.4251E-03. The convergence rate of the proposed OFDA and FDA, as in Figure 12 for the PVM model, OFDA has a quicker convergence rate than FDA.

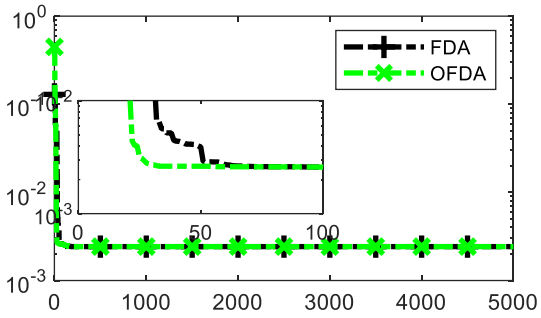


Fig. 12. The convergence curves of both the FDA and OFDA for the PVM model.

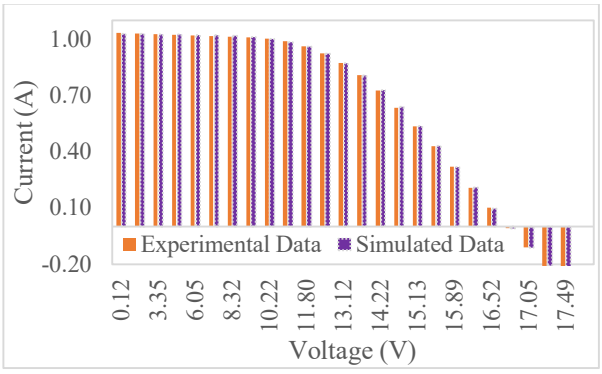


Fig. 13. (a) Current-Voltage (I-V) characteristics of PVM

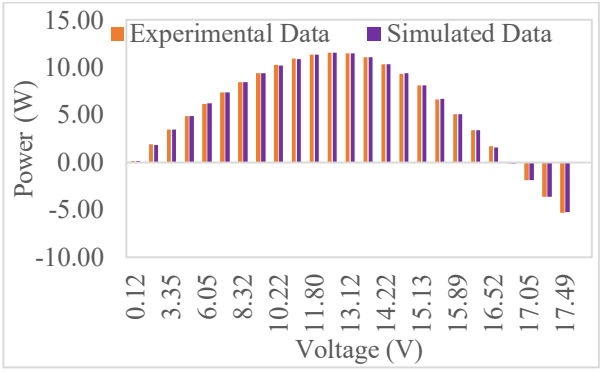


Fig. 13. (b) Power-Voltage (P-V) characteristics of PVM

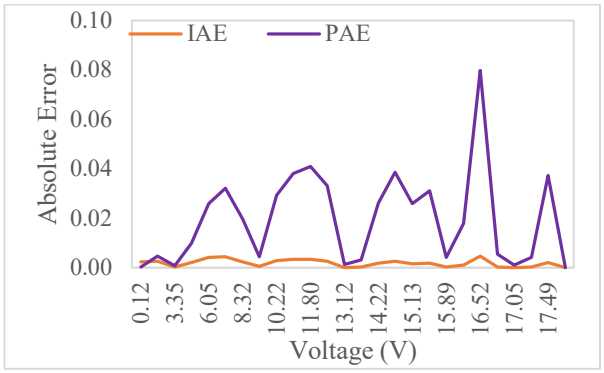


Figure 13. (c) Individual Absolute Error (IAE)

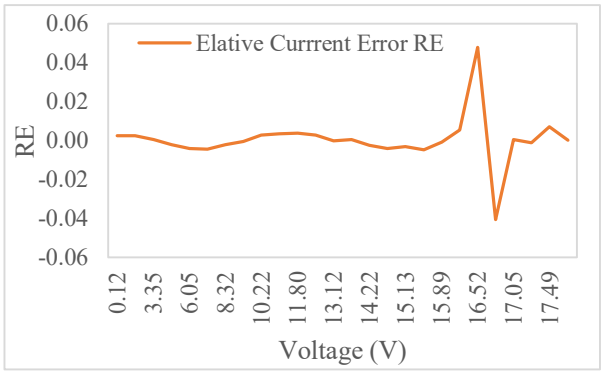


Fig. 13. (d) Relative Error (RE)

Fig. 13. The error index of the experimental and simulated current data for the PVM.

Table 11 shows the root-mean-squared error (RMSE) minimum, maximum, mean, and standard deviation throughout 30 iterations to evaluate the OFDA's effectiveness. As expected, the OFDA performs the best for Mean and Std compared with other well-known algorithms. The Mean of the OFDA is identical to the MLSBA [23], PGJAYA [27], EJADE [38], HDE [43], FDA, and OFDA. The Std. of the OFDA is very close to the EJADE [38], HDE [43], FDA, and OFDA and superior to other well-known algorithms. According to the results reported above, we may conclude that OFDA has the potential to be an effective technique for identifying the PVM parameters.

The OFDA-obtained PVM optimum parameters are shown in Table 11; the calculated I-V and P-V data are computed using these values. Table 13 displays the Individual Absolute Error (IAE), whereas Figure 13 shows the various characteristic curves among the measured and calculated data. The IAE values for the current are lower than 4.8328E-03, and the IAE values for power are lower than 7.9858E-02, which can be found in Table 11. Current and power levels calculated using the OFDA are demonstrated to agree with experimental measurements in Figure 13. All of this evidence points to the specified parameters being correct.

Table 10. The PVM results of extracted parameter values of OFDA and other well-known algorithms

Algorithm	I_{ph} (A)	I_{sd} (A)	R_s(Ω)	R_p(Ω)	n	RMSE
IJAYA [20]	1.0305	3.4703E+00	1.2016	977.3752	48.6298	**2.4251E-03**
MLBSA [23]	1.0305	3.4823E+00	1.2013	981.9823	48.3428	**2.4251E-03**
PGJAYA [27]	1.0305	3.4818E+00	1.2013	981.8545	48.6424	**2.4251E-03**
EJADE [38]	1.0305	3.4823E+00	1.2013	981.9824	48.6428	**2.4251E-03**
GWOCS [32]	1.0305	3.4650E+00	1.2019	982.7566	48.6237	**2.4251E-03**
DSCSE [42]	1.0305	3.4823E-06	1.2013	981.9820	48.6428	**2.4251E-03**
HDE [43]	1.0305	3.4823E-06	0.0334	27.27728	1.35119	**2.4251E-03**
MSSA [44]	1.0319	3.2840E+00	1.2056	841.3210	48.4036	**2.4251E-03**
OLGBO [45]	1.0305	3.4823E-06	1.2013	981.9830	48.6428	**2.4251E-03**
IMFOL [46]	1.0305	3.5151E-06	1.2003	992.2600	48.6788	**2.4251E-03**
FDA	1.0305	3.4823E-06	1.2013	981.9823	48.6428	**2.4251E-03**
OFDA	1.0305	3.4823E-06	1.2013	981.9824	48.6428	**2.4251E-03**

Table 11. The PVM statistical results of the OFDA and other well-known algorithms

Algorithm	Min	Max	Mean	Std
IJAYA [20]	2.4251E-03	2.4393E-03	2.4289E-03	3.7755E-06
MLBSA [23]	2.4508E-03	2.4253E-03	2.4251E-03	4.3368E-08
PGJAYA [27]	2.4251E-03	2.4268E-03	2.4251E-03	3.0714E-07
EJADE [38]	2.4251E-04	2.4251E-04	2.4251E-04	3.2700E-17
GWOCS [32]	2.4251E-03	2.4275E-03	2.4261E-03	1.1967E-06
DSCSE [42]	2.4251E-03	3.0034E-03	2.4444E-03	1.0558E-04
HDE [43]	2.4251E-03	2.4251E-03	2.4251E-03	3.1541E-17
MSSA [44]	2.4200E-03	2.7800E-03	2.5400E-03	1.7500E-06
OLGBO [45]	2.4251E-03	2.4378E-03	2.4255E-03	2.3312E-06
IMFOL [46]	2.4252E-03	2.7425E-01	1.8996E-01	1.0359E-01
FDA	2.4251E-03	2.4251E-03	2.4251E-03	3.0236E-17
OFDA	2.4251E-03	2.4251E-03	2.4251E-03	**2.5188E-17**

Table 12. The absolute error (IAE) values of PVM

Experimental Data		Simulated Data		Simulated Data	
V (V)	I (A)	Isim (A)	I_IAE (A)	P (W)	P_IAE (W)
0.1248	1.0315	1.029119	2.3808E-03	0.128434	2.9713E-04
1.8093	1.0300	1.027381	2.6189E-03	1.858841	4.7384E-03
3.3511	1.0260	1.025742	2.5820E-04	3.437363	8.6526E-04
4.7622	1.0220	1.024107	2.1072E-03	4.877003	1.0035E-02
6.0538	1.0180	1.022292	4.2918E-03	6.188750	2.5982E-02
7.2364	1.0155	1.019931	4.4307E-03	7.380626	3.2062E-02
8.3189	1.0140	1.016363	2.3631E-03	8.455023	1.9658E-02

9.3097	1.0100	1.010496	4.9615E-04	9.407416	4.6190E-03
10.2163	1.0035	1.000629	2.8710E-03	10.222726	2.9331E-02
11.0449	0.9880	0.984548	3.4516E-03	10.874238	3.8123E-02
11.8018	0.9630	0.959522	3.4783E-03	11.324083	4.1050E-02
12.4929	0.9255	0.922839	2.6612E-03	11.528933	3.3246E-02
13.1231	0.8725	0.872600	9.9662E-05	11.451213	1.3079E-03
13.6983	0.8075	0.807274	2.2574E-04	11.058285	3.0922E-03
14.2221	0.7265	0.728336	1.8365E-03	10.358474	2.6119E-02
14.6995	0.6345	0.637138	2.6380E-03	9.365610	3.8777E-02
15.1346	0.5345	0.536213	1.7131E-03	8.115370	2.5927E-02
15.5311	0.4275	0.429511	2.0113E-03	6.670783	3.1238E-02
15.8929	0.3185	0.318774	2.7448E-04	5.066251	4.3623E-03
16.2229	0.2085	0.207390	1.1105E-03	3.364459	1.8015E-02
16.5241	0.1010	0.096167	4.8328E-03	1.589076	7.9858E-02
16.7987	-0.0080	-0.008325	3.2539E-04	-0.139856	5.4661E-03
17.0499	-0.1110	-0.110936	6.3518E-05	-1.891456	1.0830E-03
17.2793	-0.2090	-0.209247	2.4727E-04	-3.615646	4.2726E-03
17.4885	-0.3030	-0.300864	2.1364E-03	-5.261653	3.7363E-02

5. Conclusion

In this paper, the FDA uses opposition-based learning to overcome the limitations of the original FDA. The opposition-based learning in OFDA speeds up the FDA algorithm and improves its performance. The performance of the proposed OFDA approach was analysed by extracting PV parameters; the performance of the OFDA approach has been assessed on many modules, including SDM, DDM, and PVM. Many popular methods have been used to evaluate OFDA's performance, and the findings have been compared to those of IJAYA, MLSBA, PGJAYA, EJADE, GWOCS, DSCSE, HDE, MSSA, OLGBO, MFO, IMFOL, and OFDA. The results demonstrate the superiority of the OFDA method in terms of statistical results, accuracy, consistency, and speed. Consequently, the proposed OFDA can be applied as an effective alternative solution to the problem of PV model parameter extraction.

References

[1] M. A. El-Dabah, R. A. El-Sehiemy, H. M. Hasanien, and B. Saad, "Photovoltaic model parameters identification using an innovative optimization algorithm," IET Renew. Power Gener., vol. 17, pp. 1783–1796, 2023.

[2] M. Cakir, I. Cankaya, I. Garip, and I. Colak, "Advantages of Using Renewable Energy Sources in Smart Grids," in 10th Int. Conf. Smart Grid (icSmartGrid), 2022, pp. 436–439.

[3] G. Xiong, J. Zhang, D. Shi, L. Zhu, X. Yuan, and Z. Tan, "Winner-leading competitive swarm optimizer with dynamic Gaussian mutation for parameter extraction of solar photovoltaic models," Energy Convers. Manag., vol. 206, Art. no. 112450, 2020.

[4] M. A. El-Dabah, R. A. El-Sehiemy, H. M. Hasanien, B. Saad, "Photovoltaic model parameters identification using Northern Goshawk Optimization algorithm," Energy. 2023 Jan 1;262.

[5] Z. Garip, "Parameters estimation of three-diode photovoltaic model using fractional-order Harris Hawks optimization algorithm," Optik (Stuttg). 2023 Feb 1;272.

[6] C. Yang, C. Su, H. Hu, M. Habibi, H. Safarpour, A. M. Khadimallah, "Performance optimization of photovoltaic and solar cells via a hybrid and efficient chimp algorithm," Solar Energy. 2023 Mar 15; 253:343–59.

[7] R. Mohamed, M. Abdel-Basset, K. M. Sallam, I. M. Hezam, A. M. Alshamrani, I. A. Hameed "Novel hybrid kepler optimization algorithm for parameter estimation of photovoltaic modules," Sci Rep. 2024 Dec 1;14(1).

[8] W. Al Abri, R. Al Abri, H. Yousef, and A. Al-Hinai, "A Global MPPT Based on Bald Eagle Search Technique for PV System Operating under Partial Shading Conditions," in 10th Int. Conf. Smart Grid (icSmartGrid), 2022, pp. 325–332.

[9] M. V. Da Rocha, L. P. Sampaio, and S.A.O. Da Silva, "Comparative analysis of ABC, Bat, GWO and PSO algorithms for MPPT in PV systems," in 8th Int. Conf. Renew. Energy Res. Appl. (ICRERA), 2019, pp. 347–352.

[10] K. Sundareswaran, V. Kumar, S. Palani, "Application of a combined particle swarm optimization and perturb and observe method for MPPT in PV systems under partial shading conditions," Renew Energy. 2015 Mar 1; 75:308–17.

[11] F. J. Toledo, J. M. Blanes, and V. Galiano, "Two-Step Linear Least-Squares Method for Photovoltaic Single-Diode Model Parameters Extraction," IEEE Trans. Ind. Electron., vol. 65, no. 8, pp. 6301–6308, Aug. 2018.

[12] D. Izci, S. Ekinci, A.G. Hussien, "Efficient parameter extraction of photovoltaic models with a novel enhanced prairie dog optimization algorithm," Sci Rep. 2024 Dec 1;14(1).

[13] L. L. Jiang, D. L. Maskell, and J.C. Patra, "Parameter estimation of solar cells and modules using an improved adaptive differential evolution algorithm," Appl. Energy, vol. 112, pp. 185–193, 2013.

[14] V. Khanna, B. Das, D. Bisht, and P. Singh, "A three diode model for industrial solar cells and estimation of solar cell parameters using PSO algorithm," Renew. Energy, vol. 78, pp. 105–113, 2015.

[15] C. Chellaswamy and R. Ramesh, "Parameter extraction of solar cell models based on adaptive differential evolution algorithm," Renew. Energy, vol. 97, pp. 823–837, 2016.

[16] A. R. Jordehi, "Time varying acceleration coefficients particle swarm optimization (TVACPSO): A new optimization algorithm for estimating parameters of PV cells and modules," Energy Convers. Manag., vol. 129, pp. 262–274, 2016.

[17] R. Sarjila, K. Ravi, J. B. Edward, K. S. Kumar, and A. Prasad, "Parameter Extraction of Solar Photovoltaic Modules Using Gravitational Search Algorithm," J. Electr. Comput. Eng., vol. 2016, Art. no. 9209863, 2016.

[18] Y. Zhang, P. Lin, Z. Chen, and S. Cheng, "A Population Classification Evolution Algorithm for the Parameter Extraction of Solar Cell Models," Int. J. Photoenergy, vol. 2016, Art. no. 2975313, 2016.

[19] P. Lin, S. Cheng, W. Yeh, Z. Chen, and L. Wu, "Parameters extraction of solar cell models using a modified simplified swarm optimization algorithm," Solar Energy, vol. 144, pp. 594–603, 2017.

[20] T. V. Luu and N. S. Nguyen, "Parameters extraction of solar cells using modified JAYA algorithm," Optik, vol. 203, Art. no. 164034, 2020.

[21] R. Muralidharan, "Parameter extraction of solar photovoltaic cells and modules using current–voltage characteristics," Int. J. Ambient Energy, vol. 38, no. 5, pp. 509–513, 2016.

[22] X. Gao, Y. Cui, J. Hu, G. Xu, Z. Wang, J. Qu, and H. Wang, "Parameter extraction of solar cell models using improved shuffled complex evolution algorithm," Energy Convers. Manag., vol. 157, pp. 460–479, 2018.

[23] K. Yu, J. Liang, B. Qu, Z. Cheng, and H. Wang, "Multiple learning backtracking search algorithm for estimating parameters of photovoltaic models," Appl. Energy, vol. 226, pp. 408–422, 2018.

[24] G. Xiong, J. Zhang, X. Yuan, D. Shi, and Y. He, "Application of Symbiotic Organisms Search Algorithm for Parameter Extraction of Solar Cell Models," Appl. Sci., vol. 8, no. 11, Art. no. 2155, 2018.

[25] B. Subudhi and R. Pradhan, "Bacterial Foraging Optimization approach to parameter extraction of a photovoltaic module," IEEE Trans. Sustain. Energy, vol. 9, no. 1, pp. 381–389, Jan. 2018.

[26] V. J. Chin and Z. Salam, "Coyote optimization algorithm for the parameter extraction of photovoltaic cells," Solar Energy, vol. 194, pp. 656–670, 2019.

[27] K. Yu, B. Qu, C. Yue, S. Ge, X. Chen, and J. Liang, "A performance-guided JAYA algorithm for parameters identification of photovoltaic cell and module," Appl. Energy, vol. 237, pp. 241–257, 2019.

[28] R.Z. Caglayan, K. Kayisli, N. Zhakiyev, A. Harrouz, and I. Colak, "A Review of Hybrid Renewable Energy Systems and MPPT Methods," Int. J. Smart Grid, vol. 6, no. 3, pp. 72–78, Sep. 2022.

[29] S. Li, W. Gong, X. Yan, C. Hu, D. Bai, L. Wang, and L. Gao, "Parameter extraction of photovoltaic models using an improved teaching-learning-based optimization," Energy Convers. Manag., vol. 186, pp. 293–305, 2019.

[30] T. V. Luu and N. S. Nguyen, "Parameters extraction of solar cells using modified JAYA algorithm," Optik, vol. 203, Art. no. 164034, 2020.

[31] J. Liang, K. Qiao, K. Yu, S. Ge, B. Qu, R. Xu, and K. Li, "Parameters estimation of solar photovoltaic models via a self-adaptive ensemble-based differential evolution," Solar Energy, vol. 207, pp. 336–346, 2020.

[32] W. Long, S. Cai, J. Jiao, M. Xu, and T. Wu, "A new hybrid algorithm based on grey wolf optimizer and cuckoo search for parameter extraction of solar photovoltaic models," Energy Convers. Manag., vol. 203, Art. no. 112243, 2020.

[33] X. Jian and Z. Weng, "A logistic chaotic JAYA algorithm for parameters identification of photovoltaic cell and module models," Optik, vol. 203, Art. no. 164041, 2020.

[34] M. H. Qais, H. M. Hasanien, and S. Alghuwainem, "Parameters extraction of three-diode photovoltaic model using computation and Harris Hawks optimization," Energy, vol. 195, Art. no. 117040, 2020.

[35] H. Chen, S. Jiao, M. Wang, A. A. Heidari, and X. Zhao, "Parameters identification of photovoltaic cells and modules using diversification-enriched Harris hawks optimization with chaotic drifts," J. Cleaner Prod., vol. 244, Art. no. 118778, 2020.

[36] H. M. Ridha, A. A. Heidari, M. Wang, and H. Chen, "Boosted mutation-based Harris hawks optimizer for parameters identification of single-diode solar cell

models," Energy Convers. Manag., vol. 209, Art. no. 112660, 2020.

[37] M. Naeijian, A. Rahimnejad, S.M. Ebrahimi, N. Pourmousa, and S.A. Gadsden, "Parameter estimation of PV solar cells and modules using Whippy Harris Hawks Optimization Algorithm," Energy Rep., vol. 7, pp. 4047–4063, 2021.

[38] S. Li, Q. Gu, W. Gong, and B. Ning, "An enhanced adaptive differential evolution algorithm for parameter extraction of photovoltaic models," Energy Convers. Manag., vol. 205, Art. no. 112443, 2020.

[39] M. Yesilbudak and M. Colak, "Efficient Parameter Estimation of Double Diode-Based PV Cell Model Using Marine Predators Algorithm," in 10th Int. Conf. Renew. Energy Res. Appl. (ICRERA), 2021, pp. 376–380.

[40] M. Colak and S. Balci, "Parameter Estimation of Photovoltaic System Using Marine Predators Optimization Algorithm-Based Multilayer Perceptron," in 11th Int. Conf. Renew. Energy Res. Appl. (ICRERA), 2022, pp. 540–545.

[41] W. Long, T. Wu, J. Jiao, M. Tang, and M. Xu, "Refraction-learning-based whale optimization algorithm for high-dimensional problems and parameter estimation of PV model," Eng. Appl. Artif. Intell., vol. 89, Art. no. 103457, 2020.

[42] W. Zhou, P. Wang, A.A. Heidari, X. Zhao, H. Turabieh, M. Mafarja, and H. Chen, "Metaphor-free dynamic spherical evolution for parameter estimation of photovoltaic modules," Energy Rep., vol. 7, pp. 5175–5202, 2021.

[43] D. Wang, X. Sun, H. Kang, Y. Shen, and Q. Chen, "Heterogeneous differential evolution algorithm for parameter estimation of solar photovoltaic models," Energy Rep., vol. 8, pp. 4724–4746, 2022.

[44] M. Yaghoubi, M. Eslami, M. Noroozi, H. Mohammadi, O. Kamari, and S. Palani, "Modified Salp Swarm Optimization for Parameter Estimation of Solar PV Models," IEEE Access, vol. 10, pp. 110181–110194, 2022.

[45] S. Yu, A. A. Heidari, G. Liang, C. Chen, H. Chen, and Q. Shao, "Solar photovoltaic model parameter estimation based on orthogonally-adapted gradient-based optimization," Optik, vol. 252, Art. no. 168513, 2022.

[46] M. Qaraad, S. Amjad, N.K. Hussein, M. Badawy, S. Mirjalili, and M.A. Elhosseini, "Photovoltaic parameter estimation using improved moth flame algorithms with local escape operators," Comput. Electr. Eng., vol. 106, Art. no. 108603, 2023.

[47] C. Kumar, T.D. Raj, M. Premkumar, and T.D. Raj, "A new stochastic slime mould optimization algorithm for the estimation of solar photovoltaic cell parameters," Optik, vol. 223, Art. no. 165277, 2020.

[48] H. M. Ridha, C. Gomes, and H. Hizam, "Estimation of photovoltaic module model's parameters using an improved electromagnetic-like algorithm," Neural Comput. Appl., vol. 32, no. 16, pp. 12627–12642, 2020.

[49] M. U. N. Khursheed, M. A. Alghamdi, M. F. Nadeem Khan, A. K. Khan, I. Khan, A. Ahmed, A. T. Kiani, and M. A. Khan, "PV Model Parameter Estimation Using Modified FPA with Dynamic Switch Probability and Step Size Function," IEEE Access, vol. 9, pp. 42027–42044, 2021.

[50] M. Li, C. Li, Z. Huang, J. Huang, G. Wang, and P.X. Liu, "Spiral-based chaotic chicken swarm optimization algorithm for parameters identification of photovoltaic models," Soft Comput., vol. 25, no. 20, pp. 12875–12898, 2021.

[51] H. Karami, M. V. Anaraki, S. Farzin, and S. Mirjalili, "Flow Direction Algorithm (FDA): A Novel Optimization Approach for Solving Optimization Problems," Comput. Ind. Eng., vol. 156, Art. no. 107224, 2021.

[52] R. Panda, M. Swain, M. K. Naik, S. Agrawal, and A. Abraham, "A Novel Practical Decisive Row-Class Entropy-Based Technique for Multilevel Threshold Selection Using Opposition Flow Directional Algorithm," IEEE Access, vol. 10, pp. 110473–110484, 2022.

[53] A. Maheshwari, Y.R. Sood, and S. Jaiswal, "Flow direction algorithm-based optimal power flow analysis in the presence of stochastic renewable energy sources," Electr. Power Syst. Res., vol. 216, Art. no. 109087, 2023.

[54] W. L. Cheng, K. M. Ang, W. H. Lim, S. S. Tiang, M. C. Chiong, C. K. Ang, L. Pan, C. H. Wong, "Flow Direction Algorithm for Feature Selection," in Advances in Intelligent Manufacturing and Mechatronics, M.A. Abdullah., Eds. Singapore: Springer, 2023, pp. 1–12.

[55] Y. Fan, S. Zhang, Y. Wang, D. Xu, and Q. Zhang, "An Improved Flow Direction Algorithm for Engineering Optimization Problems," Mathematics, vol. 11, no. 9, Art. no. 2217, 2023.

[56] H. R. Tizhoosh, "Opposition-Based Learning: A New Scheme for Machine Intelligence," in Int. Conf. Comput. Intell. Modelling, Control Autom. (CIMCA) and Int. Conf. Intell. Agents, Web Technol. Internet Commerce (IAWTIC'06), Vienna, Austria, 2005, pp. 695–701.

[57] S. Gupta and K. Deep, "An Efficient Grey Wolf Optimizer with Opposition-Based Learning and Chaotic Local Search for Integer and Mixed-Integer Optimization Problems," Arab J Sci Eng, vol. 44, pp. 7277–7296, 2019.